Humoral signatures of Caspr2-antibody spectrum disorder track with clinical phenotypes and outcomes

Paula Terroba-Navajas, Marianna Spatola, Omar Chuquisana, Bastien Joubert, Juna de Vries, Andre Dik, Laura Marmolejo, Friederike Jönsson, Gordan Lauc, Stjepana Kovac, et al.

Med

Humoral signatures of Caspr2-antibody spectrum disorder track with clinical phenotypes and outcomes

Graphical abstract

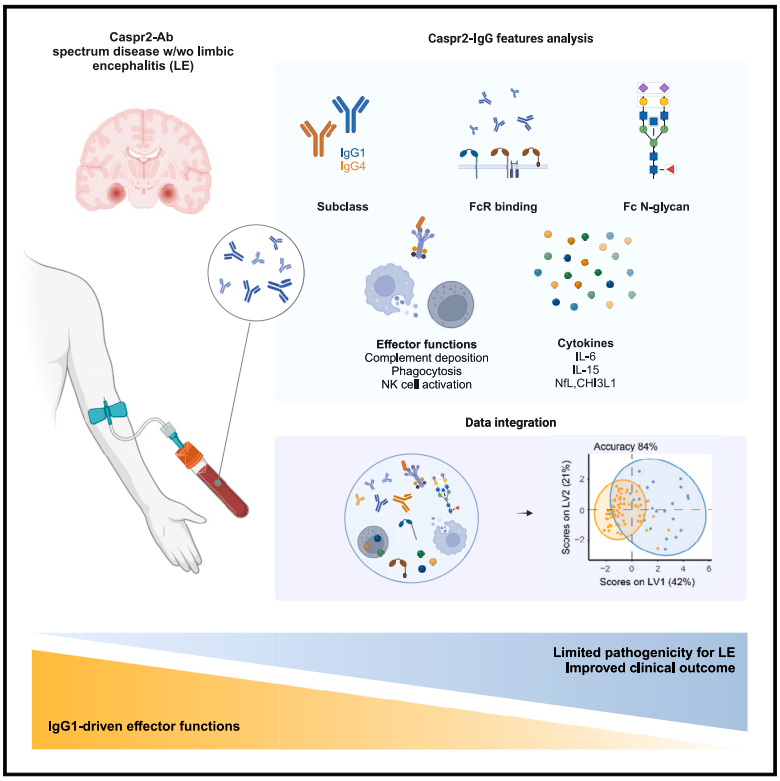

Highlights

- IgG4 and IgG1 Abs against Caspr2 occur in a broad spectrum of neurological syndromes
- Features of Caspr2-Abs can be attributed to distinct clinical phenotypes
- Caspr2-limbic encephalitis tracks with a pro-inflammatory IgG1 Fc-driven biosignature
- Occurrence of Caspr2-IgG1, in addition to IgG4, predicts poorer clinical outcome

Authors

Paula Terroba-Navajas, Marianna Spatola, Omar Chuquisana, ..., Maarten J. Titulaer, Jérôme Honnorat, Jan D. Lünemann

Correspondence

marianna.spatola@gmail.com (M.S.), jan.luenemann@ukmuenster.de (J.D.L.)

In brief

Terroba-Navajas et al. show that biophysical and functional features of auto-antibodies targeting Caspr2, expressed in neurons of the central and peripheral nervous system, are associated with distinct clinical syndromes within the spectrum of Caspr2-Ab-associated disorders. A strong pro-inflammatory Ab signature tracks with severe brain inflammation and poorer outcomes.

Translation to Patients

Terroba-Navajas et al., 2025, Med 6, 1–12
February 14, 2025
Published by Elsevier Inc.
https://doi.org/10.1016/j.medj.2024.09.004

CellPress

Please cite this article in press as: Terroba-Navajas et al., Humoral signatures of Caspr2-antibody spectrum disorder track with clinical phenotypes and outcomes, Med (2024), https://doi.org/10.1016/j.medj.2024.09.004

Med

CellPress
OPEN ACCESS

Article

Humoral signatures of Caspr2-antibody spectrum disorder track with clinical phenotypes and outcomes

Paula Terroba-Navajas,[1,13] Marianna Spatola,[2,12,13,*] Omar Chuquisana,[1] Bastien Joubert,[3,4,5] Juna M. de Vries,[6] Andre Dik,[1] Laura Marmolejo,[2] Friederike Jönsson,[7] Gordan Lauc,[8,9] Stjepana Kovac,[1] Harald Prüss,[10,11] Heinz Wiendl,[1] Maarten J. Titulaer,[6] Jérôme Honnorat,[3,4] and Jan D. Lünemann[1,14,*]

[1]Department of Neurology with Institute of Translational Neurology, University Hospital Münster, Münster, Germany
[2]Institut d'Investigacions Biomèdiques August Pi i Sunyer (IDIBAPS), Hospital Clínic, Universitat de Barcelona, Barcelona, Spain
[3]French Reference Center on Paraneoplastic Neurological Syndromes and Autoimmune Encephalitis, Hospices Civils de Lyon, Hôpital Neurologique, Lyon, France
[4]MeLiS - UCBL - CNRS UMR 5284 - INSERM U1314, Université de Lyon, Université Claude Bernard Lyon 1, Lyon, France
[5]Service de Neurologie, Centre Hospitalier Lyon Sud, Hospices Civils de Lyon, Lyon, France
[6]Department of Neurology, Erasmus University Medical Center, Rotterdam, the Netherlands
[7]CNRS & Institut Pasteur, Université Paris Cité, INSERM UMR1222, Antibodies in Therapy and Pathology, 75015 Paris, France
[8]Faculty of Pharmacy and Biochemistry, University of Zagreb, Ante Kovačića 1, Zagreb, Croatia
[9]Genos, Ltd., Borongajska Cesta 83H, Zagreb, Croatia
[10]Department of Neurology and Experimental Neurology, Charité-Universitätsmedizin Berlin, Corporate Member of Freie Universität Berlin, Humboldt-Universität zu Berlin and Berlin Institute of Health, Charitéplatz 1, Berlin, Germany
[11]German Center for Neurodegenerative Diseases (DZNE) Berlin, Berlin, Germany
[12]Caixa Research Institute, Barcelona, Spain
[13]These authors contributed equally
[14]Lead contact
*Correspondence: marianna.spatola@gmail.com (M.S.), jan.luenemann@ukmuenster.de (J.D.L.)
https://doi.org/10.1016/j.medj.2024.09.004

CONTEXT AND SIGNIFICANCE Antibodies (Abs) against contactin-associated protein-like 2 (Caspr2), expressed in neurons of the central and peripheral nervous system, are found in patients with a broad spectrum of neurological symptoms. How Caspr2-Ab functions translate into clinical syndromes is incompletely understood. By combining systems immunology with high-dimensional characterization of physical and functional Ab features, Terroba-Navajas et al. identify biosignatures that track with distinct clinical presentations of Caspr2-Ab-associated disorders and the potential of Caspr2-Abs to induce limbic encephalitis, a severe autoimmune brain disease with subacute onset, memory and cognitive deficits, and seizures. Therapeutic approaches targeting these pro-inflammatory Ab functions might potentially restrain Caspr2-Ab-induced pathology and improve clinical outcomes.

SUMMARY

Background: Immunoglobulin (Ig) G4 auto-antibodies (Abs) against contactin-associated protein-like 2 (Caspr2), a transmembrane cell adhesion protein expressed in the central and peripheral nervous system, are found in patients with a broad spectrum of neurological symptoms. While the adoptive transfer of Caspr2-specific IgG induces brain pathology in susceptible rodents, the mechanisms by which Caspr2-Abs mediate neuronal dysfunction and translate into clinical syndromes are incompletely understood.
Methods: We use a systems-level approach combined with high-dimensional characterization of Ab-associated immune features to deeply profile humoral biosignatures in patients with Caspr2-Ab-associated neurological syndromes.
Findings: We identify two signatures strongly associated with two major clinical phenotypes, limbic encephalitis (LE) and predominant peripheral nerve hyperexcitability without LE (non-LE). Caspr2-IgG Fc-driven pro-inflammatory features, characterized by increased binding affinities for activating Fcγ receptors (FcγRs) and C1q, along with a higher prevalence of IgG1-class Abs, in addition to IgG4, are strongly associated with LE.

Please cite this article in press as: Terroba-Navajas et al., Humoral signatures of Caspr2-antibody spectrum disorder track with clinical phenotypes and outcomes, Med (2024), https://doi.org/10.1016/j.medj.2024.09.004

Both the occurrence of Caspr2-specific IgG1 and higher serum levels of interleukin (IL)-6 and IL-15, along with increased concentrations of biomarkers reflecting neuronal damage and glial cell activation, are associated with poorer clinical outcomes at 1-year follow-up.

Conclusions: The presence of IgG1 isotypes and Fc-mediated effector functions control the pathogenicity of Caspr2-specific Abs to induce LE. Biologics targeting FcR function might potentially restrain Caspr2-Ab-induced pathology and improve clinical outcomes.

Funding: This study was funded by a German-French joint research program supported by the German Research Foundation (DFG) and the Agence Nationale de la Recherche (ANR) and by the Interdisciplinary Centre for Clinical Research (IZKF) Münster.

INTRODUCTION

Contactin-associated protein-like 2 (Caspr2) is a transmembrane cell adhesion protein of the neurexin family that is expressed in neurons of the central and peripheral nervous system. It is required for the proper localization of voltage-gated potassium channels (VGKCs) at the juxtaparanodes of myelinated axons.[1,2] Antibodies (Abs) to VGKC were initially reported in patients with limbic encephalitis (LE), neuromyotonia, and Morvan syndrome.[3,4] As the clinical spectrum emerged, it became clear that the Abs were not directed against VGKC subunits but rather to associated proteins: either leucine-rich glioma-inactivated1 (LGI1) or Caspr2.[5,6] The occurrence of Abs directed to Caspr2 is associated with a broad spectrum of neurological symptoms and signs, such as cognitive disturbance, seizures, cerebellar dysfunction, peripheral nerve hyperexcitability (PNH), and dysautonomia. While patients can suffer from signs and symptoms related to the full spectrum of a disease, symptoms can be allocated to two leading clinical core syndromes: (1) LE, affecting the central nervous system with memory disorders and temporal lobe seizures, or (2) PNH syndrome, characterized by muscular hyperactivity, being either restricted to the peripheral nervous system or presenting with additional encephalopathic and dysautonomic symptoms as Morvan's syndrome.[7,8]

Patients' Caspr2-Abs, which target the extracellular domain (ECD) of the protein,[9] are detectable in the peripheral blood and frequently in the cerebrospinal fluid (CSF). Caspr2-Abs are usually immunoglobulin (Ig) G4 isotypes, although Caspr2-specific IgG1 can additionally be detected in up to two-thirds of patients.[10] Caspr2-Abs have been demonstrated to be directly pathogenic in both *in vitro* and *in vivo* models. Pathogenic effects of Caspr2-specific Abs include blockade of Caspr2-related cell-to-cell interactions,[11] internalization of Caspr2 following auto-Ab-mediated crosslinking,[12] and induction of clinical disease features in rodents infused intracerebrally with patients' Abs.[13–15] Apart from these direct effects of the Abs on their targets, Abs also have the capacity to activate several effector functions by innate immune cells. Recent studies suggested a role for innate immune activation, including microglia and complement activation at the postsynaptic membrane,[16] potentially resulting in the loss of Caspr2 and neuronal dysfunction.[17] Overall, the mechanisms by which Caspr2-Ab-mediated immune functions contribute to the evolution of clinical syndromes and the heterogeneity of clinical phenotypes remain poorly understood. Furthermore, no biomarkers are available to predict or define clinical severity and disease course. The goal of the present study was to systematically profile the biophysical and functional landscape of Caspr2-specific Abs using an unbiased, high-throughput systems serology platform and identify humoral correlates for human Caspr2-Ab-associated clinical disease features and outcomes.

RESULTS

Biosignatures of Caspr2-specific Abs can be attributed to clinical phenotypes

In this multicenter retrospective study, we included 88 individuals with Caspr2-Ab spectrum disorder presenting with LE or predominant PNH without LE (hereafter referred to as non-LE phenotype [non-LE]) as clinical core syndromes (Figure 1A; Table S1). The prevalence of clinical phenotypes and the distribution of sex, age, and tumor association are representative of reported real-world cohorts.[8,18]

Using a systems serology approach, we first comprehensively assessed biophysical and functional features of Caspr2-specific Abs in patients with LE vs. non-LE, such as IgG effector functions (antibody-dependent complement deposition [ADCD], cellular phagocytosis [ADCP], and natural killer cell activation [ADNKA]), Fc gamma receptor (FcγR) binding affinities (FcγR 2A, 2B, 3A, 3B, and C1q components), and the presence of IgG1-Caspr2 isotypes in addition to Caspr2-specific IgG4. Features were analyzed independently of Ab titers. Since the sugar moiety attached to the IgG constant heavy 2 (C_H2) domain (Figure 1B) is critical to determine the capacity of IgG molecules to execute effector functions,[19] we additionally determined IgG-Fc glycosylation profiles.

We observed striking differences in Ab-associated biosignatures, specifically related to the capacity for eliciting Fc-mediated effector functions (Figures 1C and 1D). To fully capture the differences between LE and non-LE Ab profiles, we applied least absolute shrinkage and selection operator (LASSO) feature selection with partial least squares discriminant analysis (PLS-DA) (model validation $p < 0.001$ by permutated test, accuracy: 84% by cross-validation; Figure 1E). This approach effectively condensed the initial 19 Ab features into a minimal subset necessary to distinguish between the two groups. The model used seven key features to resolve the two groups. These features included binding capacity to FcγR3A and FcγR2A, ADCP, and the presence of Caspr2-IgG1 isotypes (in addition to IgG4) that were enriched in patients with LE, while features related to terminal IgG-Fc glycosylation, such as the presence of S2, G2, and S1 sugar moieties, were enriched in non-LE patients (Figure 1E).

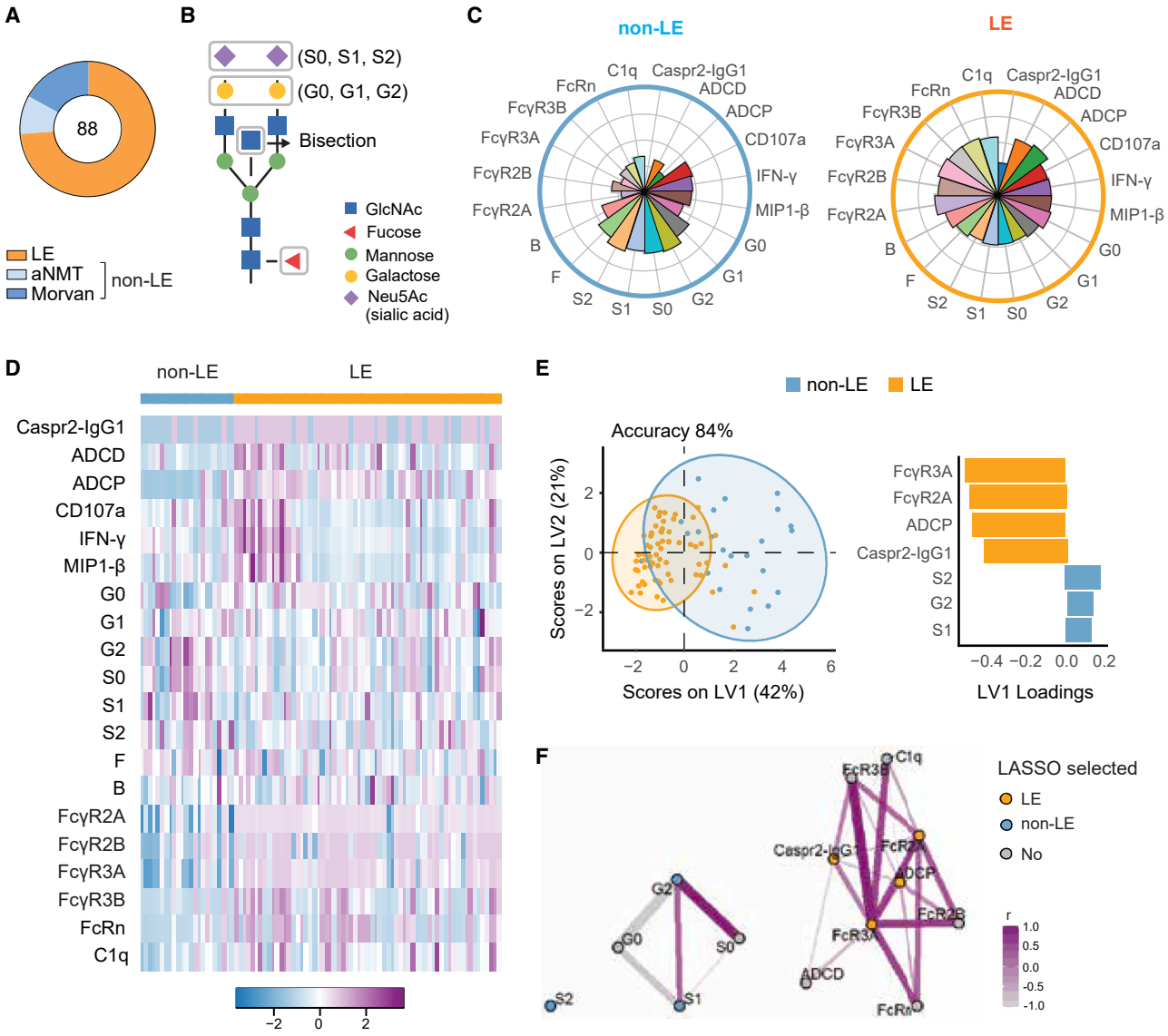

Figure 1. Caspr2-specific Ab features discriminate between LE and non-LE phenotypes

(A) Clinical syndromes in patients with Caspr2-Abs-associated spectrum disease in our cohort. LE, limbic encephalitis; aNMT, acquired neuromyotonia; Morvan, Morvan syndrome.

(B) Scheme of the IgG N-linked glycan structure. The base glycan structure is pictured, and the main variable sugar residues are presented inside the boxes.

(C) Flower plots summarizing the data from Caspr2-Ab-mediated effector functions (antibody-dependent complement deposition: ADCD; phagocytosis: ADCP; and NK activation [ADNKA]: CD107a, interferon [IFN]-γ, MIP-1β), Fc-glycosylation (G0, G1, S1, S2, F, B), and capacity to bind Fc gamma receptors (FcγRs; FcγR2A, FcγR2B, FcγR3A, FcγR3B, FcRn) and complement component (C1q) in LE serum (n = 65) compared to non-LE (n = 23). The length of the petal represents the mean percentile rank for the indicated feature.

(D) Heatmap of Z scored values of Caspr2-Ab-mediated effector functions (antibody-dependent complement deposition: ADCD; phagocytosis: ADCP; and NK activation [ADNKA]: CD107a, IFN-γ, MIP-1β), Fc-glycosylation (G0, G1, S1, S2, F, B), and capacity to bind FcγRs (FcγR2A, FcγR2B, FcγR3A, FcγR3B, FcRn) and complement component (C1q) in all LE (n = 65) and non-LE (n = 23).

(E) Partial least squares discriminant analysis (PLS-DA) in LASSO-selected features was used to resolved LE and non-LE based on Ab features. Dots represent individual samples (orange: LE; blue: non-LE). Model accuracy of 84% by cross-validation, model validation $p < 0.001$ by permutation test. The LASSO-selected features were ranked based on their variable importance in projection (VIP). Bars represent Ab features enriched in non-LE (blue) vs. LE (orange).

(F) Correlation network between LASSO-selected features in LE (orange dots), non-LE (blue dots), and other features (gray dots). Spearman r test was performed with Benjamini-Hochberg correction for multiple comparisons. Only correlations with $r > 0.5$ and $p < 0.05$ are shown. The color and width of edges are proportional to the correlation coefficient (r). G, galactose; S, sialic acid; F, fucose; B, bisecting GlcNc.

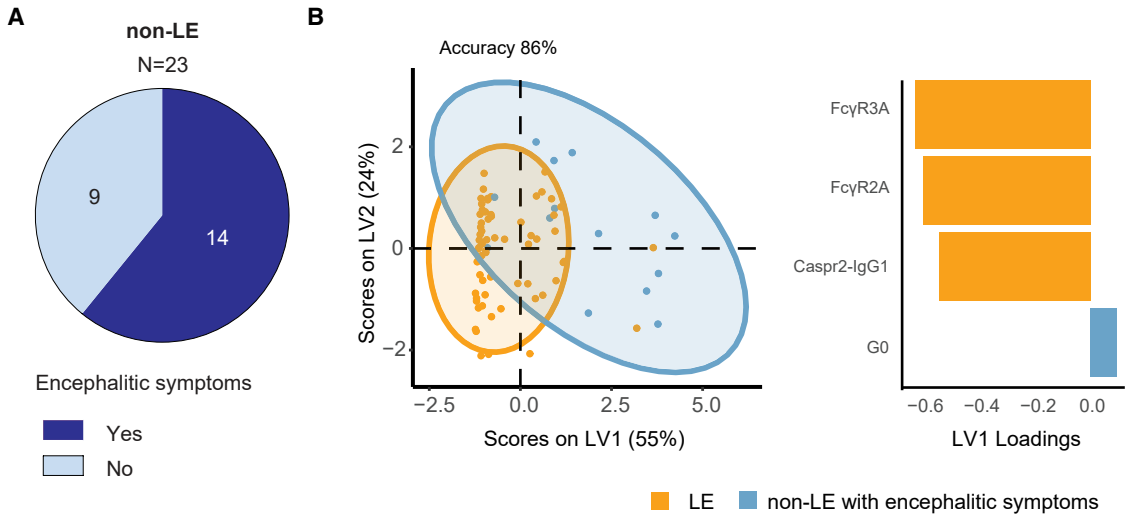

Figure 2. Caspr2-specific Ab features discriminate between LE and non-LE syndromes associated with signs of CNS involvement

(A) Frequency of encephalitic symptoms (anterograde amnesia, behavioral problems, episodic or permanent ataxia, cognitive disturbance, hyperkinetic movement disorders, nocturnal hallucinations) in Caspr2-Ab$^+$ patients not diagnosed with LE.

(B) Partial least squares discriminant analysis (PLS-DA) in LASSO-selected features was used to resolve LE and non-LE with encephalitic symptoms based on Ab features. Dots represent individual samples (orange: LE; blue: non-LE). Model accuracy of 86% by cross-validation, model validation $p < 0.001$ by permutation test. The LASSO selected features were ranked based on their variable importance in projection (VIP). Bars represent Ab features enriched in non-LE (blue) vs. LE (orange).

To assess the features that were biologically related to the LASSO-selected profiles, we built correlation networks based on Spearman correlation coefficients (Figure 1F). We observed that the LASSO-selected features enriched in LE positively correlated with binding to other FcγRs, as well as with ADCD and C1q binding. Importantly, the presence of Caspr2-IgG1 (in addition to IgG4) also positively correlated with FcγR binding and Ab effector functions (ADCP and ADCD), indicating an overall higher functionality of Abs in the LE phenotype. On the other hand, glycan features enriched in non-LE only correlated with other glycan profiles, not with FcR binding or functions (Figure 1F).

Encephalitic symptoms in Caspr2-Ab-positive (Caspr2-Ab$^+$) patients can also occur in the absence of LE. In our cohort, 14/23 patients not diagnosed with LE showed symptoms compatible with CNS involvement (anterograde amnesia, behavioral problems, episodic or permanent ataxia, cognitive disturbance, hyperkinetic movement disorders, nocturnal hallucinations) (Figure 2A). The LASSO/PLS-DA-selected key features that distinguish patients with LE from non-LE patients with encephalitic symptoms were similar to those identified for LE vs. non-LE, namely binding affinities to FcγR3A and FcγR2A, the presence of Caspr2-IgG1 isotypes (in addition to IgG4), enriched in patients with LE patients, while IgG-Fc glycosylation feature G0 was enriched in non-LE patients with encephalitic symptoms (model validation $p < 0.001$ by permutation test, accuracy: 86% by cross-validation; Figure 2B). These data support the notion that the identified pro-inflammatory Ab signature is associated with LE.

In agreement with the multivariate analysis, univariate analysis confirmed the higher capacity of Caspr2-Abs to induce Fc-mediated effector functions, such as ADCP and ADCD, and bind FcγRs and C1q in LE samples compared to non-LE samples (Figure 3A). Correlation among Ab features, in particular between FcγR binding capacities and Ab-mediated functions, was higher in patients with LE (Figure 3B), indicating a more coordinated humoral response in LE compared to non-LE. Frequencies of glycovariants carrying terminal sialic acid and galactose sugar moieties tended to be higher in non-LE patients, while frequencies of IgG glycovariants lacking terminal galactosylation, i.e., G0, were significantly increased in patients with Caspr2-Ab$^+$ LE (Figure 3C).

We next developed receiver operating characteristic (ROC) curves to explore the performance, in terms of sensitivity and specificity, of the seven LASSO-selected immune features to discriminate between LE and non-LE. Importantly, the seven Ab features depicted in Figure 1E (presence of Caspr2-IgG1, higher binding capacity to FcγR3A and FcγR2A, higher ADCP, G2, S1 and S2 glycoforms frequency) showed an outstanding discriminating performance (area under the curve [AUC] = 0.911) between the two dominant clinical phenotypes (Figure 3D).

IgG-Fc and IgG-Fab glycosylation profiles in Caspr2-Ab spectrum disorder

We additionally compared IgG-Fc-glycan profiles in patients with Caspr2-Ab$^+$ disorder with demographically matched healthy controls. Frequencies of Fc N-glycans carrying one or two galactose and two sialic acid residues were significantly reduced in Caspr2-Ab$^+$ patients (Figure 4A).

We extended our analysis to include the IgG-Fab glycan profiles. Although the biological significance of IgG-Fab glycan profiles remains uncertain, we observed similar differences in IgG-Fc and IgG-Fab glycoprofiles between the abovementioned Caspr2 phenotypes (Figure S1) and a higher coordination of IgG Fc- and Fab-glycosylation features in patients with LE (Figure 4B).

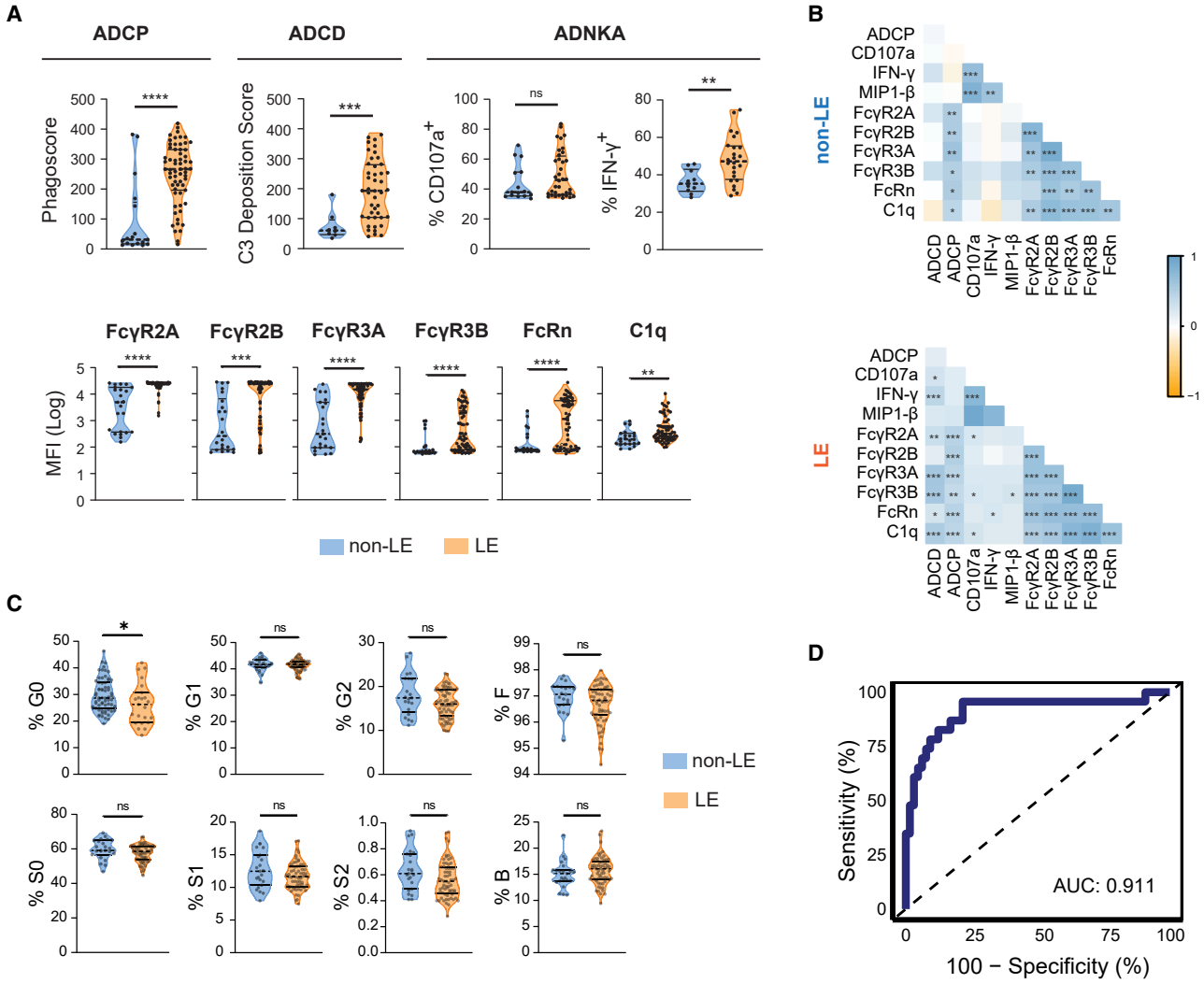

Figure 3. Pro-inflammatory signature of Caspr2-Abs in LE

(A) Univariate comparison Caspr2-Ab-mediated effector functions (antibody-dependent complement deposition: ADCD; phagocytosis: ADCP; and NK activation [ADNKA]: CD107a, IFNγ, MIP-1β) and capacity to bind Fc receptors (FcγRs; FcγR2A, FcγR2B, FcγR3A, FcγR3B, FcRn) and complement component (C1q) in non-LE ($n = 23$) vs. LE ($n = 65$) phenotypes. The dashed line in the violin plots indicate the median per group, and solid lines indicate quartiles. Each dot represents an individual patient. Mann-Whitney test was used for statistical comparisons between groups; p values indicate statistical significance (*$p \leq 0.05$, **$p \leq 0.001$, ***$p \leq 0.001$, and ****$p \leq 0.0001$).

(B) Correlation matrix across features showed in (A) according to phenotype (non-LE vs. LE). Correlation strength is proportional to color intensity. Spearman r correlation was used with Benjamini-Hochberg correction for multiple comparisons; p values indicate statistical significance (*$p \leq 0.05$, **$p \leq 0.001$, ***$p \leq 0.001$).

(C) Univariate comparison of Fc glycosylation levels between non-LE and LE phenotypes within the Caspr2-Abs-associated disease cohort. The dashed line indicates median per group, and solid lines indicate quartiles. Each dot represents an individual patient. Mann-Whitney test was used for statistical comparisons between groups; p values indicate statistical significance (*$p \leq 0.05$, **$p \leq 0.001$, ***$p \leq 0.001$, and ****$p \leq 0.0001$).

(D) ROC curve was used to evaluate the accuracy of LASSO-selected Ab-associated immune features to discern between non-LE and LE phenotypes. AUC, area under the curve.

Overall, these data suggest that Caspr2-Abs signatures track with clinical phenotypes and point to unique Ab features in patients with LE, characterized by highly coordinated humoral response with increased FcR binding affinities, Fc-mediated effector functions, and presence of the IgG1 subclass (in addition to IgG4), along with pro-inflammatory IgG-Fc glycoforms lacking terminal galactosylation.

Presence of Caspr2-IgG1 tracks with stronger Fc-mediated effector functions

Caspr2-Ab-associated neurological syndromes are traditionally thought to be IgG4 mediated, although some patients also harbor IgG1 Caspr2-specific Abs.[11] Caspr2-IgG1 Abs, in addition to Caspr2-IgG4, could be detected in about two-thirds of the patients included in our study (Table S1; Figure 5A). To further

Please cite this article in press as: Terroba-Navajas et al., Humoral signatures of Caspr2-antibody spectrum disorder track with clinical phenotypes and outcomes, Med (2024), https://doi.org/10.1016/j.medj.2024.09.004

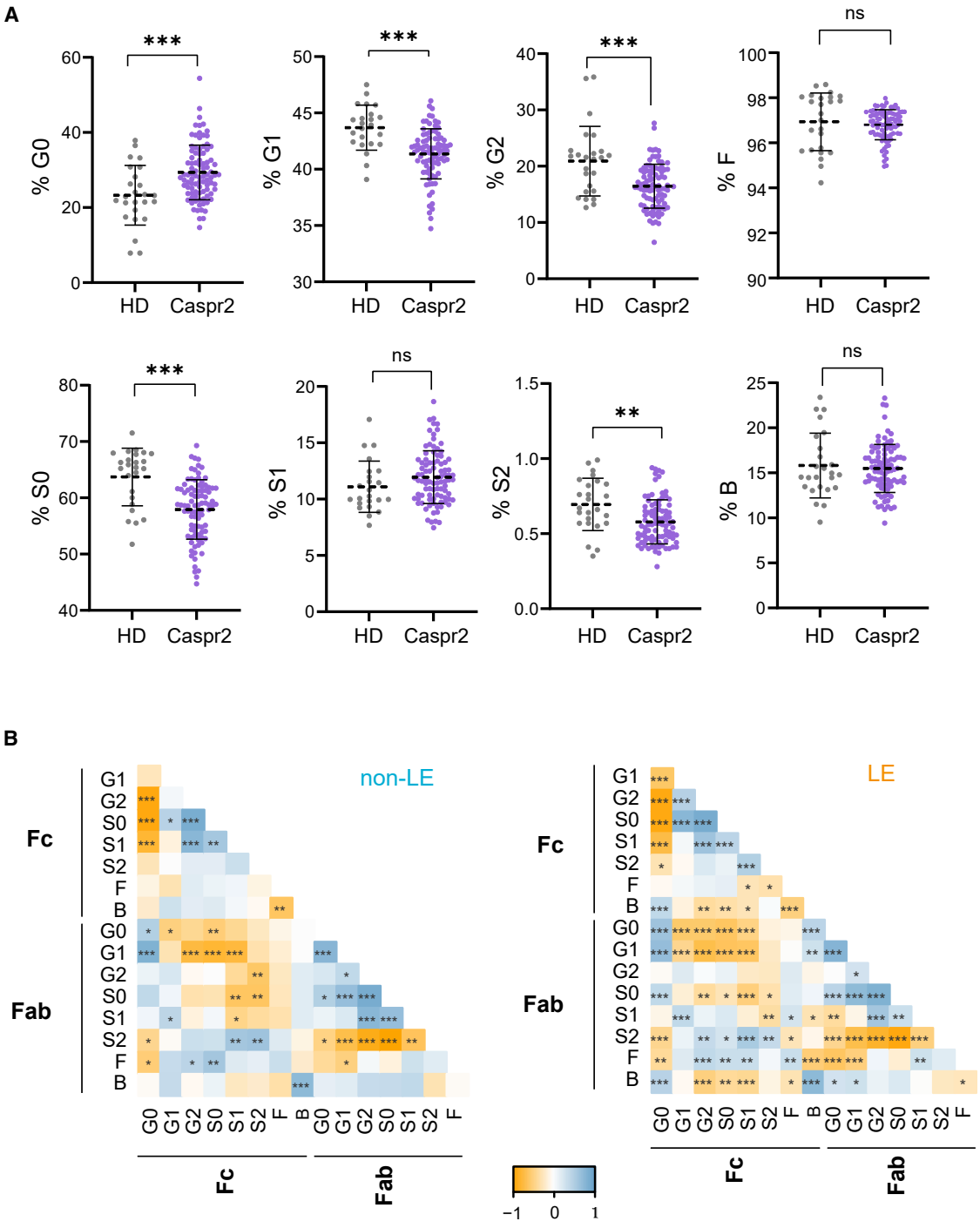

Figure 4. IgG glycan composition

(A) Univariate comparison of Fc glycosylation levels between healthy donors (HDs) and Caspr2 sera. The dashed line indicates the mean per group, and solid lines indicate SD. Each dot represents an individual patient. Mann-Whitney test was used for statistical comparisons between groups; *p* values indicate statistical significance (*$p \leq 0.05$, **$p \leq 0.001$, ***$p \leq 0.001$).

(B) Correlation matrix across levels of Fc and Fab glycan composition in non-LE (top) and LE (bottom). Correlation strength is proportional to color intensity. Spearman r correlation was used with Benjamini-Hochberg correction for multiple comparisons; *p* values indicate statistical significance (*$p \leq 0.05$, **$p \leq 0.001$, ***$p \leq 0.001$). G, galactose; S, sialic acid; F, fucose; B, bisecting GlcNc.

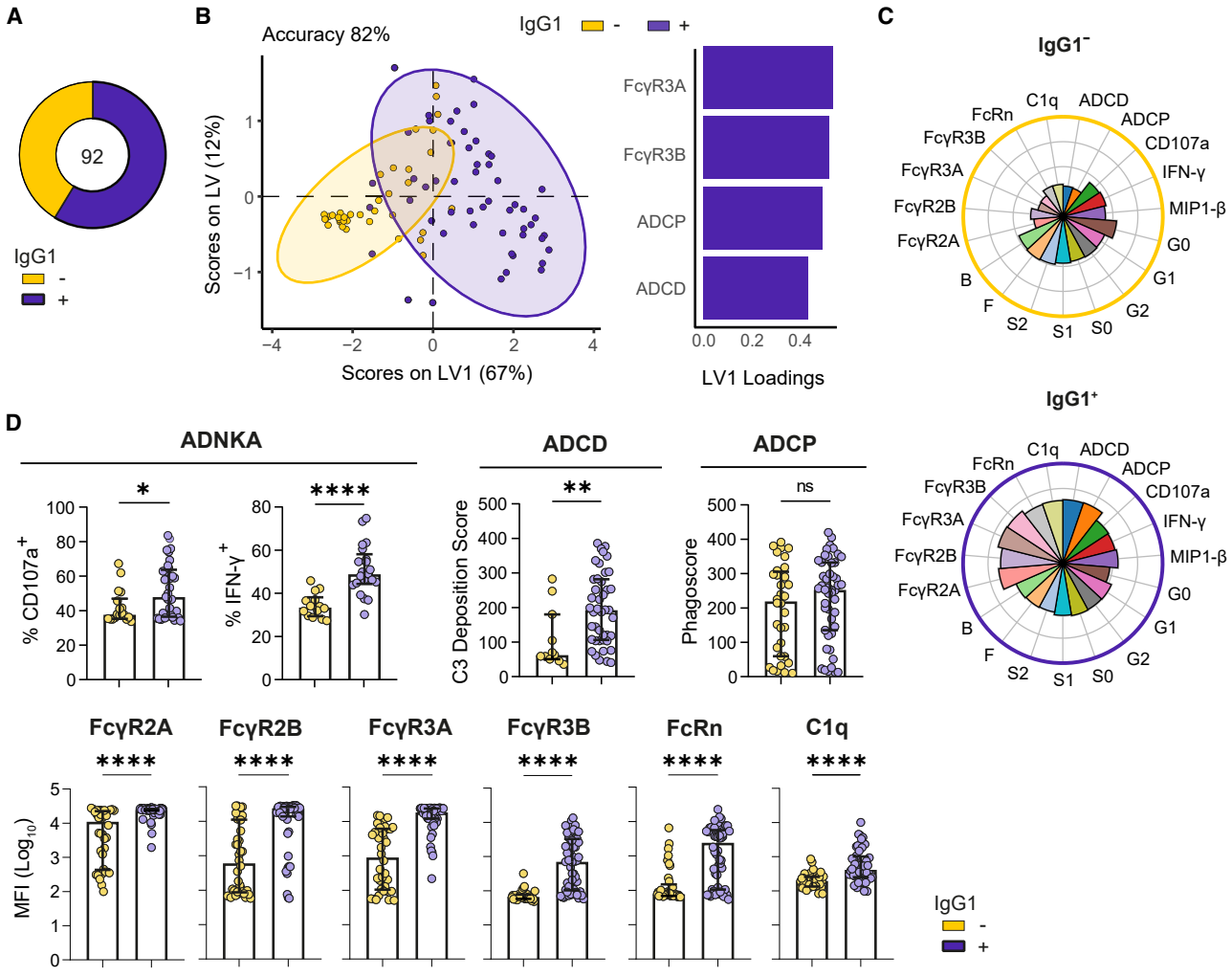

Figure 5. Caspr2-IgG1 Fc-driven pro-inflammatory features

(A) Frequency of Caspr2-specific IgG1 in sera (in addition to IgG4 isotype).

(B) Partial least squares discriminant analysis (PLS-DA) in LASSO-selected features showing the differences on Ab signatures depending on the presence of Caspr2-specific IgG1 Abs. Dots represent individual samples (yellow: Caspr2-IgG1^{-}; blue: Caspr2-IgG1^{+}). Model accuracy of 81% by cross-validation, model validation $p < 0.001$ by permutation test. The LASSO-selected features were ranked based on their variable importance in projection (VIP). Bars represent Ab features enriched in Caspr2-IgG1^{+} (purple).

(C) Flower plots showing Caspr2-Ab-mediated effector functions (complement deposition: ADCD; phagocytosis: ADCP; and NK activation [ADNKA]: CD107a, IFNγ, MIP-1β), Fc-glycosylation (G0, G1, S1, S2, F, B), and capacity to bind Fc receptors (FcγRs; FcγR2A, FcγR2B, FcγR3A, FcγR3B, FcRn) and complement component (C1q) in Caspr2-IgG1 negative ($n = 38$) and positive ($n = 54$) sera. The length of the petal represents the mean percentile rank for the indicated feature.

(D) Univariate analysis of Ab effector functions (antibody-dependent complement deposition: ADCD; phagocytosis: ADCP; and NK activation [ADNKA]: CD107a, IFNγ) and capacity to bind FcγRs (FcγR2A, FcγR2B, FcγR3A, FcγR3B, FcRn) and complement component (C1q) in the presence or absence of IgG1 Caspr2-Ab isotypes. The bar plot indicate the median per group, and solid lines indicate quartiles. Each dot represents an individual patient. Mann-Whitney test was used for statistical comparisons between groups, p values indicate statistical significance (*$p \leq 0.05$, **$p \leq 0.001$, ***$p \leq 0.001$, and ****$p \leq 0.0001$).

explore the potential effects of Caspr2-IgG1 isotypes, we performed a multivariate analysis to study the Ab features that are mainly associated with the presence or absence of additional Caspr2-IgG1. Using a PLS-DA/LASSO approach, we observed a good separation between the IgG1^{+} and IgG1^{-} groups (model validation $p < 0.001$ by permutation test, model accuracy: 82%; Figure 5B). This model identified FcRγ3A, FcRγ3B, ADCP, and ADCD, all enriched in the Caspr2-IgG1 Ab^{+} group as the main drivers of the separation (Figure 5B). In accordance with these results, we observed, at a univariate level, a higher capacity to activate innate immune functions (in particular ADCD and ADNKA) and bind to Fc receptors in the presence of Caspr2-IgG1 Abs (Figures 5C and 5D).

Serological signatures defining clinical outcomes

Disease severity and functional outcomes in autoimmune encephalitides and Caspr2-Ab^{+} spectrum disorder are mainly assessed using the modified Rankin scale (mRS), a 7-point disability scale

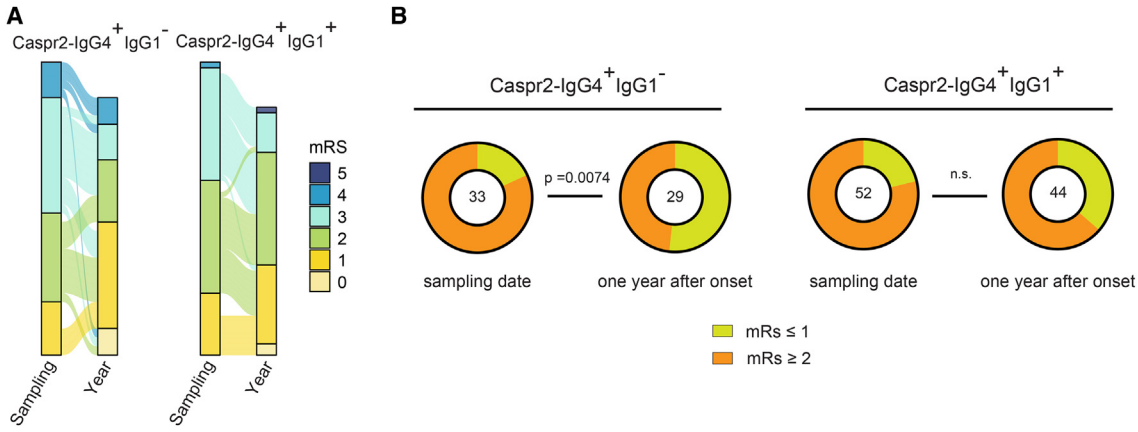

Figure 6. Presence of Caspr2-IgG1 is associated with poorer clinical outcomes

(A) Summary of matched mRS scores at sampling date and after 1-year follow-up in Caspr2-IgG1$^-$ and Caspr2-IgG1$^+$sera.

(B) Percentage of patients with different mRS scores at sampling and after 1-year follow-up based on the presence or absence of Caspr2-specific IgG1 (in addition to IgG4 isotype).

measuring the degree of disability or dependence in the daily activities with possible scores ranging from 0 (no symptoms) to 6 (death). Most patients with Caspr2-Ab$^+$ spectrum disorder benefit from immunotherapy, but the clinical outcome is variable. We therefore investigated whether serological features in patients with Caspr2-IgG$^+$ syndromes are associated with clinical outcomes 1 year upon onset of disease. The majority of the patients had a decrease in their mRS from onset to 1 year (Table S1). However, improvement was less strong in Caspr2-IgG1$^+$ patients (Figure 6A). An mRS score of one or less indicates full clinical remission (i.e., no disability, able to carry out all usual activities as before onset of disease). The proportion of subjects reaching full disease remission 1 year after onset was significantly increased in patients negative for Caspr2-IgG1 (82% vs. 48%; Figure 5B). These differences were not significant for patients who tested positive for Caspr2-IgG1 (79% vs. 64%; Figure 6B).

We additionally evaluated whether inflammation- and CNS-damage-associated serological features not directly related to IgG function correlate with clinical outcomes. To this end, we determined serum concentrations of canonical biomarkers reflecting neuroaxonal damage, such as the soluble neurofilament light chain (NfL), microglial and astroglial activation such as Chitinase-3-like 1 (CHI3L1/YKL-40), and soluble triggering receptor expressed on myeloid cells 2 (TREM2), as well as pro-inflammatory cytokines previously described to be elevated in autoimmune CNS diseases.[20,21] Serum levels of NfL, CHI3L1, interleukin (IL)-6, and IL-15 were strongly associated with poorer clinical outcomes as assessed by mRS scores 1 year after onset (Figures 7A and 7B). Thus, functional Caspr2-IgG1 responses, in addition to IgG4, track with Caspr2-LE and, along with high IL-6 and IL-15 serum levels, with poorer disease outcomes.

DISCUSSION

High-dimensional characterization of Caspr2-Ab-associated immune features identified two distinct biological signatures that were strongly associated with the two main clinical phenotypes of Caspr2-Abs-associated spectrum disease: LE and non-LE. Caspr2-IgG Fc-driven pro-inflammatory features, such as affinities for activating FcγRs, FcR-mediated phagocytosis, and complement deposition, were strongly increased in patients with LE. In line with these findings, both microglial activation and complement deposition are prominent neuropathological features in Caspr2-LE.[17,22] Activation of microglia and reactive astrocytes, which up-regulate C3 expression and mediate complement-mediated neuronal and synaptic loss, has additionally been observed upon injection of Caspr2-IgG into rodent brains, notably in the absence of overt B and T cell infiltration,[13,16] supporting the concept that FcR-mediated functions of Caspr2-IgG critically contribute to the pathology of Caspr2-LE.

IgG is the classic Ab isotype involved in T cell-dependent B cell responses, and each IgG subclass has unique properties and effector functions, with IgG1 being superior to IgG4 complexes in binding FcγRs and C1q.[23–25] Caspr2-Ab-associated autoimmune syndromes are traditionally categorized as IgG4 mediated due to IgG4 being the predominant subclass. However, Caspr2-IgG1 species are additionally observed in up to two-third of cases, as confirmed in our cohort.[10]

Polarization of IgG subclasses is determined by cytokine milieu and upstream signals from the encounter of T helper cells with antigen-presenting cells across the immunological synapse.[26] Notably, the presence of HLA-DRB1*11:01 is strongly associated with Caspr2-LE[27] while carrier frequencies for this allele are reported to be similar in non-LE patients compared to healthy volunteers.[8] Such immunogenetic features might inform T cell specificities and functions at disease initiation and contribute to the polarization of Caspr2-specific IgG responses toward an IgG1 or IgG4 response and subsequent evolution of clinical phenotypes. In patients with co-occurrence of both isotypes, Caspr2-IgG1-mediated pathogenic functions likely act in concert with IgG4-mediated effects[11,12] in contributing to neuronal dysfunction and increased neuropathology.

Apart from Ab isotypes, the sugar moiety attached to the C_H2 domain is critical for maintaining both the pro-inflammatory and

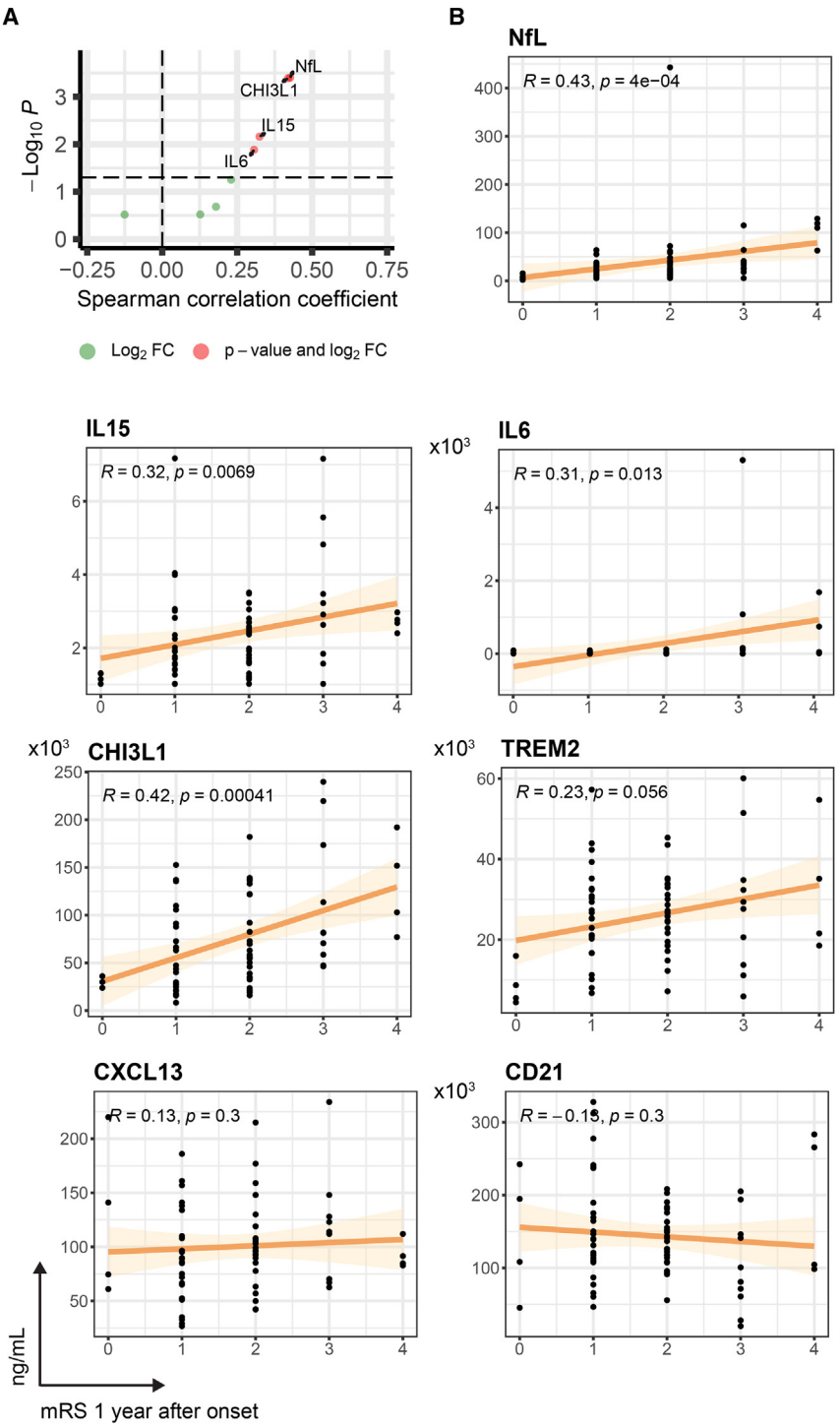

Figure 7. Increased serum IL-6 and IL-15 along with biomarkers for glial cell activation and axonal damage correlate with clinical outcomes

(A) Volcano plot shows the correlation of each sera marker with mRS score at 1-year after onset. Spearman correlation coefficients are indicated in the x axis, and the statistical significance is indicated in the y axis ($-\log_{10}$[p value]). Values above the black dashed line indicate statistically significant correlations (adjusted $p < 0.05$ by Benjamini-Hochberg correction for multiple comparisons).

(B) mRS scores at 1-year follow-up (linear regression [blue line] with its confidence interval [blue area]) vs. concentration of selected sera markers (ng/mL). Each dot is one sample. Spearman correlation coefficient (R) and associated p value (p) are indicated in the top left corner. mRS scores of 4 and 5 are plotted together as mRS = 4.

anti-inflammatory effector functions of IgG molecules.[19] A decrease in the level of IgG galactosylation, and hence an increase in the abundance of agalactosylated G0 glycoforms, is one of the most prominent and established changes in IgG glycosylation at the level of total-serum and antigen-specific IgGs in a broad spectrum of chronic inflammatory and autoimmune diseases, such as rheumatoid arthritis (RA), systemic lupus erythematosus (SLE), autoimmune vasculitis, and Crohn's disease.[19] In agreement with these findings, frequencies of IgG Fc-glycoforms carrying one or two galactose and two sialic acid residues were significantly reduced in patients with Caspr2-Ab spectrum disorder compared to demographically matched healthy controls, and agalactosylated G0 glycoforms were increased in patients with Caspr2-Ab$^+$ LE compared to those without LE. Whether a lack of IgG-Fc terminal galactose or sialic acid residues translates into higher functional pro-inflammatory activity of Abs or merely reflects chronic inflammatory processes without actively contributing to autoimmune disease development and severity has not been conclusively clarified. Data obtained in mice, however, suggest that a lack of terminal galactosylation or sialylation changes the IgG structure and increases the affinity for activating FcγRs.[28–34]

Higher disease severity at 1-year follow-up strongly correlated with increased NfL protein levels, reflecting neuronal damage, as well as with markers of astroglial activation, such as CHI3L1. Increased levels of IL-6 and IL-15 after onset were additionally associated with higher disability at 1-year follow-up examinations. While increased serum levels of neuronal and glial biomarkers are frequently detected in many CNS inflammatory and neurodegenerative diseases,[35,36] a prominent role for IL-6 with elevated serum and CSF levels and therapeutic benefits of blocking IL-6 function has specifically been described for the two most frequent IgG-mediated CNS autoimmune diseases,

i.e., aquaporin-4 (AQP4)-Ab$^+$, neuromyelitis optica spectrum disorder (NMOSD), and myelin oligodendrocyte glycoprotein (MOG)-Ab-associated disorder (MOGAD).[20,21] IL-6 is thought to contribute to both aforementioned diseases by promoting Ab-secreting cell (plasmablasts) survival,[37] enhancing pro-inflammatory T cell differentiation and activation,[38] and reducing the integrity and functionality of the blood-brain barrier.[39] IL-15 stimulates the generation and function of natural killer (NK) and memory CD8$^+$ T cells, among other immune cells, and is constitutively up-regulated in several autoimmune diseases, including multiple sclerosis (MS).[40–45] In patients with Caspr2-Ab$^+$ LE, a role for CD8$^+$ T cells in aggravating disease pathology has been suggested based on case series describing the enrichment of CD8$^+$ T cells in the CSF[46] and in temporal lobe biopsies,[47] but the exact contribution of T cells or NK cells in Caspr2-Ab$^+$ spectrum disorder remains incompletely understood.

Taken together, our results provide a framework for correlating biosignatures of Caspr2-specific Abs with clinical disease phenotypes. Functional Caspr2-IgG1 responses, in addition to IgG4, track with Caspr2-LE and, along with high IL-6 and IL-15 serum levels, with poorer disease outcomes, suggesting a previously unexplored role for this isotype in Caspr2-Ab-associated disease pathogenesis. Follow-up studies are required to further evaluate the predictive value of Caspr2-IgG1 responses for disability outcomes and in guiding treatment decisions.

Limitations of the study

Our study has limitations. While most patients with Caspr2-Ab spectrum disorder mainly suffer either from LE or peripheral symptoms (non-LE), a 2-fold division into these clinical phenotypes might be an oversimplification, as some patients are also affected by milder symptoms related to the full spectrum of disease. However, distinct clinical, immunogenetic,[7,8] and serological characteristics, as outlined in our study, support the concept that the evolution of the two core syndromes is driven by different immunologic mechanisms.

Given the relatively low number of samples, our exploratory study requires validation in larger cohorts of patients, ideally recruited before the start of immunotherapy and with longer-term follow-up. In addition to mRS scores, more granular clinical scales need to be developed and validated to profile disease burden and outcome for patients with Caspr2-Ab-associated syndromes.

Cellular mechanisms beyond those that are directly elicited by Caspr2-Abs and potentially shape the Ab signatures identified, such as T cell repertoire and functional analyses, were not addressed in this study. Whether clinically effective immunotherapy may overcome Fc-driven functional signatures of Caspr2-Abs also remains unclear. Thus, future systems immunology studies capturing both cellular and humoral immune features may provide further critical insights into the pathobiology of Caspr2 autoimmunity and for the design of targeted therapeutic approaches.

RESOURCE AVAILABILITY

Lead contact

Further inquiries and requests should be directed to the lead contact, Jan D. Lünemann (jan.luenemann@ukmuenster.de).

Materials availability

This study did not generate new unique reagents.

Data and code availability

- This study did not generate or report original code.
- Data reported in this paper will be shared by the lead contact upon request.
- Any additional information required to reanalyze the data reported in this paper is available from the lead contact upon request.

ACKNOWLEDGMENTS

The study was funded by a German-French joint research program supported by the German Research Foundation (DFG) and the Agence Nationale de la Recherche (ANR) (“AntibodyOMICs in CASPR2 Encephalitis” to J.D.L. and F.J.) and the Interdisciplinary Centre for Clinical Research (IZKF) Münster (to J.D.L.). M.S. receives personal research support from “la Caixa” Foundation (Junior Leader) and the Spanish National Health Institute (Instituto Carlos III, FIS 2023, PI23/01366). J.D.L. received research support by the EU Framework Programme Horizon Europe, the German Research Foundation (LU 9001-1; LU 900-4), and the Collaborative Research Centre (SFB-TRR128 “Initiating/Effector versus Regulatory Mechanisms in Multiple Sclerosis – Progress towards Tackling the Disease”). J.H. and B.J. are supported by the BETPSY project as part of the second Investissements d’Avenir programme (ANR-18-RHUS-0012) supported by a public grant overseen by the ANR. The authors thank Kerstin Stein, University Hospital Münster, for expert technical assistance. The graphical abstract was created with BioRender.com.

AUTHOR CONTRIBUTIONS

J.D.L. conceptualized the study; P.T.-N., M.S., L.M., and O.C. performed the experiments; P.T.-N. and M.S. performed the formal analysis; B.J., J.M.d.V., A.D., G.L., S.K., H.P., M.J.T., and J.H. provided the resources; P.T.-N., M.S., and J.D.L. prepared the first draft of the manuscript; and P.T.-N., M.S., O.C., B.J., J.M.d.V., A.D., L.M., F.J., G.L., S.K., H.P., H.W., M.J.T., J.H., and J.D.L. reviewed and edited the manuscript. P.T.-N. and M.S. provided further information on data oversight. P.T.-N. and J.D.L. performed statistical analysis. P.T.-N., M.S., and J.D.L. had unrestricted access to all data. All authors agreed to submit the manuscript, read and approved the final draft, and take full responsibility for its content, including the accuracy of the data.

DECLARATION OF INTERESTS

The authors declare no competing interests.

STAR★METHODS

Detailed methods are provided in the online version of this paper and include the following:

- KEY RESOURCES TABLE
- EXPERIMENTAL MODEL AND STUDY PARTICIPANT DETAILS
  - Study design and participants
- METHOD DETAILS
  - Biotinylation and coupling of the beads
  - Antibody-dependent complement deposition (ADCD)
  - Antibody-dependent cellular phagocytosis (ADCP)
  - Antibody-dependent NK cell activation (ADNKA)
  - Fc receptors (FcR) and complement C1q binding
  - Glycan analyses
  - Serologic biomarker assessment
  - Determination of Caspr2 antibody isotypes
- QUANTIFICATION AND STATISTICAL ANALYSIS

SUPPLEMENTAL INFORMATION

Supplemental information can be found online at https://doi.org/10.1016/j.medj.2024.09.004.

Received: June 13, 2024
Revised: July 15, 2024
Accepted: September 10, 2024
Published: October 10, 2024

REFERENCES

1. van Sonderen, A., Petit-Pedrol, M., Dalmau, J., and Titulaer, M.J. (2017). The value of LGI1, Caspr2 and voltage-gated potassium channel antibodies in encephalitis. Nat. Rev. Neurol. *13*, 290–301. https://doi.org/10.1038/nrneurol.2017.43.
2. Hivert, B., Pinatel, D., Labasque, M., Tricaud, N., Goutebroze, L., and Faivre-Sarrailh, C. (2016). Assembly of juxtaparanodes in myelinating DRG culture: Differential clustering of the Kv1/Caspr2 complex and scaffolding protein 4.1B. Glia *64*, 840–852. https://doi.org/10.1002/glia.22968.
3. Buckley, C., Oger, J., Clover, L., Tüzün, E., Carpenter, K., Jackson, M., and Vincent, A. (2001). Potassium channel antibodies in two patients with reversible limbic encephalitis. Ann. Neurol. *50*, 73–78. https://doi.org/10.1002/ana.1097.
4. Barber, P.A., Anderson, N.E., and Vincent, A. (2000). Morvan's syndrome associated with voltage-gated K+ channel antibodies. Neurology *54*, 771–772. https://doi.org/10.1212/wnl.54.3.771.
5. Irani, S.R., Alexander, S., Waters, P., Kleopa, K.A., Pettingill, P., Zuliani, L., Peles, E., Buckley, C., Lang, B., and Vincent, A. (2010). Antibodies to Kv1 potassium channel-complex proteins leucine-rich, glioma inactivated 1 protein and contactin-associated protein-2 in limbic encephalitis, Morvan's syndrome and acquired neuromyotonia. Brain *133*, 2734–2748. https://doi.org/10.1093/brain/awq213.
6. Lai, M., Huijbers, M.G.M., Lancaster, E., Graus, F., Bataller, L., Balice-Gordon, R., Cowell, J.K., and Dalmau, J. (2010). Investigation of LGI1 as the antigen in limbic encephalitis previously attributed to potassium channels: a case series. Lancet Neurol. *9*, 776–785. https://doi.org/10.1016/S1474-4422(10)70137-X.
7. Saint-Martin, M., Joubert, B., Pellier-Monnin, V., Pascual, O., Noraz, N., and Honnorat, J. (2018). Contactin-associated protein-like 2, a protein of the neurexin family involved in several human diseases. Eur. J. Neurosci. *48*, 1906–1923. https://doi.org/10.1111/ejn.14081.
8. Muñiz-Castrillo, S., Joubert, B., Elsensohn, M.H., Pinto, A.L., Saint-Martin, M., Vogrig, A., Picard, G., Rogemond, V., Dubois, V., Tamouza, R., et al. (2020). Anti-CASPR2 clinical phenotypes correlate with HLA and immunological features. J. Neurol. Neurosurg. Psychiatry *91*, 1076–1084. https://doi.org/10.1136/jnnp-2020-323226.
9. Olsen, A.L., Lai, Y., Dalmau, J., Scherer, S.S., and Lancaster, E. (2015). Caspr2 autoantibodies target multiple epitopes. Neurol. Neuroimmunol. Neuroinflamm. *2*, e127. https://doi.org/10.1212/NXI.0000000000000127.
10. van Sonderen, A., Ariño, H., Petit-Pedrol, M., Leypoldt, F., Körtvélyessy, P., Wandinger, K.P., Lancaster, E., Wirtz, P.W., Schreurs, M.W.J., Sillevis Smitt, P.A.E., et al. (2016). The clinical spectrum of Caspr2 antibody–associated disease. Neurology *87*, 521–528. https://doi.org/10.1212/WNL.0000000000002917.
11. Patterson, K.R., Dalmau, J., and Lancaster, E. (2018). Mechanisms of Caspr2 antibodies in autoimmune encephalitis and neuromyotonia. Ann. Neurol. *83*, 40–51. https://doi.org/10.1002/ana.25120.
12. Joubert, B., Petit-Pedrol, M., Planagumà, J., Mannara, F., Radosevic, M., Marsal, M., Maudes, E., García-Serra, A., Aguilar, E., Andrés-Bilbé, A., et al. (2022). Human CASPR2 Antibodies Reversibly Alter Memory and the CASPR2 Protein Complex. Ann. Neurol. *91*, 801–813. https://doi.org/10.1002/ana.26345.
13. Giannoccaro, M.P., Menassa, D.A., Jacobson, L., Coutinho, E., Prota, G., Lang, B., Leite, M.I., Cerundolo, V., Liguori, R., and Vincent, A. (2019). Behaviour and neuropathology in mice injected with human contactin-associated protein 2 antibodies. Brain *142*, 2000–2012. https://doi.org/10.1093/brain/awz119.
14. Manso, C., Querol, L., Mekaouche, M., Illa, I., and Devaux, J.J. (2016). Contactin-1 IgG4 antibodies cause paranode dismantling and conduction defects. Brain *139*, 1700–1712. https://doi.org/10.1093/brain/aww062.
15. Dawes, J.M., Weir, G.A., Middleton, S.J., Patel, R., Chisholm, K.I., Pettingill, P., Peck, L.J., Sheridan, J., Shakir, A., Jacobson, L., et al. (2018). Immune or Genetic-Mediated Disruption of CASPR2 Causes Pain Hypersensitivity Due to Enhanced Primary Afferent Excitability. Neuron *97*, 806–822.e10. https://doi.org/10.1016/j.neuron.2018.01.033.
16. Coutinho, E., Menassa, D.A., Jacobson, L., West, S.J., Domingos, J., Moloney, T.C., Lang, B., Harrison, P.J., Bennett, D.L.H., Bannerman, D., and Vincent, A. (2017). Persistent microglial activation and synaptic loss with behavioral abnormalities in mouse offspring exposed to CASPR2-antibodies in utero. Acta Neuropathol. *134*, 567–583. https://doi.org/10.1007/s00401-017-1751-5.
17. Körtvelyessy, P., Bauer, J., Stoppel, C.M., Brück, W., Gerth, I., Vielhaber, S., Wiedemann, F.R., Heinze, H.J., Bartels, C., and Bien, C.G. (2015). Complement-associated neuronal loss in a patient with CASPR2 antibody–associated encephalitis. Neurol. Neuroimmunol. Neuroinflamm. *2*, e75. https://doi.org/10.1212/nxi.0000000000000075.
18. Boyko, M., Au, K.L.K., Casault, C., de Robles, P., and Pfeffer, G. (2020). Systematic review of the clinical spectrum of CASPR2 antibody syndrome. J. Neurol. *267*, 1137–1146. https://doi.org/10.1007/s00415-019-09686-2.
19. Wang, T.T., and Ravetch, J.V. (2019). Functional diversification of IgGs through Fc glycosylation. J. Clin. Invest. *129*, 3492–3498. https://doi.org/10.1172/JCI130029.
20. Fujihara, K., Bennett, J.L., de Seze, J., Haramura, M., Kleiter, I., Weinshenker, B.G., Kang, D., Mughal, T., and Yamamura, T. (2020). Interleukin-6 in neuromyelitis optica spectrum disorder pathophysiology. Neurol. Neuroimmunol. Neuroinflamm. *7*, e841. https://doi.org/10.1212/NXI.0000000000000841.
21. Ringelstein, M., Ayzenberg, I., Lindenblatt, G., Fischer, K., Gahlen, A., Novi, G., Hayward-Könnecke, H., Schippling, S., Rommer, P.S., Kornek, B., et al. (2022). Interleukin-6 Receptor Blockade in Treatment-Refractory MOG-IgG-Associated Disease and Neuromyelitis Optica Spectrum Disorders. Neurol. Neuroimmunol. Neuroinflamm. *9*, e1100. https://doi.org/10.1212/NXI.0000000000001100.
22. Chuquisana, O., Strippel, C., Tröscher, A.M., Baumgartner, T., Rácz, A., Keller, C.W., Elger, C.E., Melzer, N., Kovac, S., Wiendl, H., et al. (2022). Complement activation contributes to GAD antibody-associated encephalitis. Acta Neuropathol. *144*, 381–383. https://doi.org/10.1007/s00401-022-02448-x.
23. Wang, Y., Krémer, V., Iannascoli, B., Goff, O.R.L., Mancardi, D.A., Ramke, L., de Chaisemartin, L., Bruhns, P., and Jönsson, F. (2022). Specificity of mouse and human Fcgamma receptors and their polymorphic variants for IgG subclasses of different species. Eur. J. Immunol. *52*, 753–759. https://doi.org/10.1002/eji.202149766.
24. Tao, M.H., Canfield, S.M., and Morrison, S.L. (1991). The differential ability of human IgG1 and IgG4 to activate complement is determined by the COOH-terminal sequence of the CH2 domain. J. Exp. Med. *173*, 1025–1028. https://doi.org/10.1084/jem.173.4.1025.
25. Vidarsson, G., Dekkers, G., and Rispens, T. (2014). IgG subclasses and allotypes: from structure to effector functions. Front. Immunol. *5*, 520. https://doi.org/10.3389/fimmu.2014.00520.
26. Dustin, M.L., and Choudhuri, K. (2016). Signaling and Polarized Communication Across the T Cell Immunological Synapse. Annu. Rev. Cell Dev. Biol. *32*, 303–325. https://doi.org/10.1146/annurev-cellbio-100814-125330.
27. Binks, S., Varley, J., Lee, W., Makuch, M., Elliott, K., Gelfand, J.M., Jacob, S., Leite, M.I., Maddison, P., Chen, M., et al. (2018). Distinct HLA

associations of LGI1 and CASPR2-antibody diseases. Brain *141*, 2263–2271. https://doi.org/10.1093/brain/awy109.

28. Kaneko, Y., Nimmerjahn, F., and Ravetch, J.V. (2006). Anti-inflammatory activity of immunoglobulin G resulting from Fc sialylation. Science *313*, 670–673. https://doi.org/10.1126/science.1129594.
29. Malhotra, R., Wormald, M.R., Rudd, P.M., Fischer, P.B., Dwek, R.A., and Sim, R.B. (1995). Glycosylation changes of IgG associated with rheumatoid arthritis can activate complement via the mannose-binding protein. Nat. Med. *1*, 237–243. https://doi.org/10.1038/nm0395-237.
30. Nimmerjahn, F., Anthony, R.M., and Ravetch, J.V. (2007). Agalactosylated IgG antibodies depend on cellular Fc receptors for in vivo activity. Proc. Natl. Acad. Sci. USA *104*, 8433–8437. https://doi.org/10.1073/pnas.0702936104.
31. Quast, I., Keller, C.W., Maurer, M.A., Giddens, J.P., Tackenberg, B., Wang, L.X., Münz, C., Nimmerjahn, F., Dalakas, M.C., and Lünemann, J.D. (2015). Sialylation of IgG Fc domain impairs complement-dependent cytotoxicity. J. Clin. Invest. *125*, 4160–4170. https://doi.org/10.1172/JCI82695.
32. Rademacher, T.W., Williams, P., and Dwek, R.A. (1994). Agalactosyl glycoforms of IgG autoantibodies are pathogenic. Proc. Natl. Acad. Sci. USA *91*, 6123–6127. https://doi.org/10.1073/pnas.91.13.6123.
33. Sondermann, P., Pincetic, A., Maamary, J., Lammens, K., and Ravetch, J.V. (2013). General mechanism for modulating immunoglobulin effector function. Proc. Natl. Acad. Sci. USA *110*, 9868–9872. https://doi.org/10.1073/pnas.1307864110.
34. Spatola, M., Chuquisana, O., Jung, W., Lopez, J.A., Wendel, E.M., Ramanathan, S., Keller, C.W., Hahn, T., Meinl, E., Reindl, M., et al. (2023). Humoral signatures of MOG-antibody-associated disease track with age and disease activity. Cell Rep. Med. *4*, 100913. https://doi.org/10.1016/j.xcrm.2022.100913.
35. Gill, A.J., Schorr, E.M., Gadani, S.P., and Calabresi, P.A. (2023). Emerging imaging and liquid biomarkers in multiple sclerosis. Eur. J. Immunol. *53*, e2250228. https://doi.org/10.1002/eji.202250228.
36. Bernhardt, A.M., Tiedt, S., Teupser, D., Dichgans, M., Meyer, B., Gempt, J., Kuhn, P.H., Simons, M., Palleis, C., Weidinger, E., et al. (2023). A unified classification approach rating clinical utility of protein biomarkers across neurologic diseases. EBioMedicine *89*, 104456. https://doi.org/10.1016/j.ebiom.2023.104456.
37. Jego, G., Bataille, R., and Pellat-Deceunynck, C. (2001). Interleukin-6 is a growth factor for nonmalignant human plasmablasts. Blood *97*, 1817–1822. https://doi.org/10.1182/blood.v97.6.1817.
38. Heink, S., Yogev, N., Garbers, C., Herwerth, M., Aly, L., Gasperi, C., Husterer, V., Croxford, A.L., Möller-Hackbarth, K., Bartsch, H.S., et al. (2017). Trans-presentation of IL-6 by dendritic cells is required for the priming of pathogenic T(H)17 cells. Nat. Immunol. *18*, 74–85. https://doi.org/10.1038/ni.3632.
39. Takeshita, Y., Fujikawa, S., Serizawa, K., Fujisawa, M., Matsuo, K., Nemoto, J., Shimizu, F., Sano, Y., Tomizawa-Shinohara, H., Miyake, S., et al. (2021). New BBB Model Reveals That IL-6 Blockade Suppressed the BBB Disorder, Preventing Onset of NMOSD. Neurol. Neuroimmunol. Neuroinflamm. *8*, e1076. https://doi.org/10.1212/NXI.0000000000001076.
40. Saikali, P., Antel, J.P., Pittet, C.L., Newcombe, J., and Arbour, N. (2010). Contribution of astrocyte-derived IL-15 to CD8 T cell effector functions in multiple sclerosis. J. Immunol. *185*, 5693–5703. https://doi.org/10.4049/jimmunol.1002188.
41. Schneider, R., Mohebiany, A.N., Ifergan, I., Beauseigle, D., Duquette, P., Prat, A., and Arbour, N. (2011). B cell-derived IL-15 enhances CD8 T cell cytotoxicity and is increased in multiple sclerosis patients. J. Immunol. *187*, 4119–4128. https://doi.org/10.4049/jimmunol.1100885.
42. Laurent, C., Deblois, G., Clénet, M.L., Carmena Moratalla, A., Farzam-Kia, N., Girard, M., Duquette, P., Prat, A., Larochelle, C., and Arbour, N. (2021). Interleukin-15 enhances proinflammatory T-cell responses in patients with MS and EAE. Neurol. Neuroimmunol. Neuroinflamm. *8*, e931. https://doi.org/10.1212/NXI.0000000000000931.
43. Vaknin-Dembinsky, A., Brass, S.D., Gandhi, R., and Weiner, H.L. (2008). Membrane bound IL-15 is increased on CD14 monocytes in early stages of MS. J. Neuroimmunol. *195*, 135–139. https://doi.org/10.1016/j.jneuroim.2008.01.016.
44. Richmond, J.M., Strassner, J.P., Zapata, L., Jr., Garg, M., Riding, R.L., Refat, M.A., Fan, X., Azzolino, V., Tovar-Garza, A., Tsurushita, N., et al. (2018). Antibody blockade of IL-15 signaling has the potential to durably reverse vitiligo. Sci. Transl. Med. *10*, eaam7710. https://doi.org/10.1126/scitranslmed.aam7710.
45. Benito-Miguel, M., García-Carmona, Y., Balsa, A., Pérez de Ayala, C., Cobo-Ibáñez, T., Martín-Mola, E., and Miranda-Carús, M.E. (2009). A dual action of rheumatoid arthritis synovial fibroblast IL-15 expression on the equilibrium between CD4+CD25+ regulatory T cells and CD4+CD25- responder T cells. J. Immunol. *183*, 8268–8279. https://doi.org/10.4049/jimmunol.0900007.
46. Melzer, N., Golombeck, K.S., Gross, C.C., Meuth, S.G., and Wiendl, H. (2012). Cytotoxic CD8+ T cells and CD138+ plasma cells prevail in cerebrospinal fluid in non-paraneoplastic cerebellar ataxia with contactin-associated protein-2 antibodies. J. Neuroinflammation *9*, 160. https://doi.org/10.1186/1742-2094-9-160.
47. Ünverengil, G., Vanli Yavuz, E.N., Tüzün, E., Erdağ, E., Kabadayi, S., Bilgiç, B., and Baykan, B. (2016). Brain Infiltration of Immune Cells in CASPR2-Antibody Associated Mesial Temporal Lobe Epilepsy with Hippocampal Sclerosis. Noro Psikiyatr. Ars. *53*, 344–347. https://doi.org/10.5152/npa.2016.15932.
48. Fischinger, S., Fallon, J.K., Michell, A.R., Broge, T., Suscovich, T.J., Streeck, H., and Alter, G. (2019). A high-throughput, bead-based, antigen-specific assay to assess the ability of antibodies to induce complement activation. J. Immunol. Methods *473*, 112630. https://doi.org/10.1016/j.jim.2019.07.002.
49. Ackerman, M.E., Moldt, B., Wyatt, R.T., Dugast, A.S., McAndrew, E., Tsoukas, S., Jost, S., Berger, C.T., Sciaranghella, G., Liu, Q., et al. (2011). A robust, high-throughput assay to determine the phagocytic activity of clinical antibody samples. J. Immunol. Methods *366*, 8–19. https://doi.org/10.1016/j.jim.2010.12.016.
50. Huffman, J.E., Pučić-Baković, M., Klarić, L., Hennig, R., Selman, M.H.J., Vučković, F., Novokmet, M., Krištić, J., Borowiak, M., Muth, T., et al. (2014). Comparative performance of four methods for high-throughput glycosylation analysis of immunoglobulin G in genetic and epidemiological research. Mol. Cell. Proteomics *13*, 1598–1610. https://doi.org/10.1074/mcp.M113.037465.
51. Hanic, M., Vuckovic, F., Deris, H., Bewshea, C., Lin, S., Goodhand, J.R., Ahmad, T., Trbojevic-Akmacic, I., Kennedy, N.A., Lauc, G., et al. (2023). Anti-TNF Biologicals Enhance the Anti-Inflammatory Properties of IgG N-Glycome in Crohn's Disease. Biomolecules *13*, 954. https://doi.org/10.3390/biom13060954.
52. Hanic, M., Lauc, G., and Trbojevic-Akmacic, I. (2019). N-Glycan Analysis by Ultra-Performance Liquid Chromatography and Capillary Gel Electrophoresis with Fluorescent Labeling. Curr Protoc Protein Sci *97*, e95. https://doi.org/10.1002/cpps.95.

Please cite this article in press as: Terroba-Navajas et al., Humoral signatures of Caspr2-antibody spectrum disorder track with clinical phenotypes and outcomes, Med (2024), https://doi.org/10.1016/j.medj.2024.09.004

CellPress
OPEN ACCESS

STAR★METHODS

KEY RESOURCES TABLE

REAGENT or RESOURCE	SOURCE	IDENTIFIER
Antibodies		
Anti-guinea pig complement C3 goat IgG fraction, fluorescein-conjugated	MP Biomedicals	Cat#0855385; RRID:AB_2334913
PE-Cy5 Mouse anti-human CD107a (clone H4A3)	BD Biosciences	Cat#555802; RRID:AB_396136
APC-Cy7 Mouse anti-human CD16 (clone 3G8)	BD Biosciences	Cat#557758; RRID:AB_396864
PE-Cy7 Mouse anti-human CD56 (clone B159)	BD Biosciences	Cat#557747; RRID:AB_396853
AF700 Mouse anti-human CD3 (clone UCHT-1)	BD Biosciences	Cat#557943; RRID:AB_396952
PE Mouse Anti-Human MIP-1β (clone D21-1351)	BD Biosciences	Cat#550078; RRID:AB_393549
APC Mouse Anti-Human IFN-γ (clone B27)	BD Biosciences	Cat#554702; RRID:AB_398580
Biotin Mouse Anti-Human IgG1 (clone G17-1)	BD Bioscience	Cat#555869; RRID:AB_396187
Biotin Mouse Anti-Human IgG4 (clone JDC-14)	BD Bioscience	Cat#555879; RRID:AB_396192
Biological samples		
Human serum	Recruited from tertiary hospitals in The Netherlands, France and Germany	N/A
NK cells from human buffy coats	Blood donors from University Hospital Münster, Germany	N/A
Chemicals, peptides, and recombinant proteins		
Recombinant human FcγR, FcγR2AR, FcγR2AH, FcγR2B, FcγR3AF, FcγR3AV, FcγR3B, and C1q	Duke Protein Production facility	N/A
Recombinant Human Caspr2 Protein	R&D Systems	Cat#8207-CR
Protein A/G beads (magnetic)	Thermo Fisher Scientific	Cat#26162
IdeS Protease	Promega	Cat#V7511
PNGase F	Promega	Cat#V4831
streptavidin HRP-Conjugate	Millipore	Cat#18-152
Critical commercial assays		
EZ-link Sulfo-NHS-LC-LC-Biotin	Thermo Fisher Scientific	Cat#21338
Zebra Spin Desalting Columns	Thermo Fisher Scientific	Cat#PI-89883
FluoSpheres NeutrAvidin-labeled Microspheres, 1 μm, red fluorescent (580/605), 1% solids	Thermo Fisher Scientific	Cat#F8775
FluoSpheres NeutrAvidin-labeled Microspheres, 1 μm, yellow-green fluorescent (505/515), 1% solids	Thermo Fisher Scientific	Cat#F8776
Low-Tox complement guinea pig	Cederlane	Cat#CL4051
NK cell isolation kit, Human	Miltenyi	Cat#130-092657
GolgiStop protein transport inhibitor	BD Biosciences	Cat#554724
Brefeldin A solution, 1000X	Biolegend	Cat#420601
Fix & Perm cell fixation kit & Permeabilization kit	Thermo Fisher Scientific	Cat#00-5523-00

(*Continued on next page*)

Continued

REAGENT or RESOURCE	SOURCE	IDENTIFIER
Glycan AssureHyPerformance APTS kit	Applied Biosystem	Cat#A33953
CHI3L1+TREM2	R&D Systems	Cat#SPCKC-PS-005492
CD21	R&D Systems	Cat#SPCKC-PS-000370
BLA+IL15+IL6+NFL	R&D Systems	Cat#SPCKC-PS-008574
Software and algorithms		
R version 4.3.3	R Core	https://cran.r-project.org/
Prism GraphPad Version 10.0.0	GraphPad Software Inc.	https://www.graphpad.com/
FlowJo-V10	BD Bioscience	https://www.flowjo.com/
BioRender	BioRender	https://www.biorender.com/
Code	Github	https://github.com/LoosC/systemsseRology

EXPERIMENTAL MODEL AND STUDY PARTICIPANT DETAILS

Study design and participants

Patients diagnosed with Caspr2-Ab spectrum disorder were recruited retrospectively from Université Claude Bernard Lyon1, France ($n = 61$), Erasmus University Medical Center, Rotterdam, the Netherlands ($n = 13$), Charité-Universitätsmedizin Berlin, Germany ($n = 7$) and University Hospital Münster, Germany ($n = 11$) with informed consent and under IRB-approved protocols. Participants information on sex and age was self-reported. Information on gender, race/ancestry, ethnicity, and socioeconomic status was not collected. Our study examined samples from male and female subjects. However, as this disease is known to be exceedingly prevalent in males, sex as a biological variable was not considered as there was not sufficient statistical power due to the low number of females. Diagnosis of Caspr2-Ab disease was established by clinical criteria and identification, at disease onset, of Caspr2 antibodies in serum and/or CSF samples by cell-based assays using in-house tests or commercial kits as reported.[11] Hospital Ethics Committee approval was obtained at each center, according to the Declaration of Helsinki in its current version. Clinical information (including age, sex, tumor association, type of immunotherapy, main clinical syndrome, severity and outcome) was retrieved from medical records. Disease severity was assessed by modified Rankin Scale (mRS) at sampling date and at one-year follow-up. Caspr-2 Abs were identified in all serum samples and 60 CSF samples (not determined in CSF samples from 16 patients). Caspr2-Abs were more frequently positive in the CSF of LE compared to non-LE (96% vs. 33%, $p < 0.001$) (Table S1). To avoid potential bias induced by immunotherapies, we included only immunotherapy-naïve patients and patients after a prolonged wash-out period of at least eight weeks following discontinuous pulse steroid, intravenous *immunoglobulin* or plasma exchange therapy. Patients receiving oral steroids or any other immunosuppressive therapies (like Rituximab) were excluded. For three Caspr2-Ab$^+$ patients the clinical data is not available and one presents with propriospinal myoclonus. Serum samples at disease onset were available for antibody analyses, were stored at −80°C until use and thawed on ice prior to experiments. Each sample was run in duplicate, and results were obtained by averaging duplicates. Serum samples from age- and sex-matched healthy donors (HD) from University Hospital Münster, Germany ($n = 10$) were used as negative controls.

METHOD DETAILS

Biotinylation and coupling of the beads

Biotinylation of recombinant Human Caspr2 (rhCaspr2) Protein (#8207-CR, R&D Systems) was carried out using EZ-link Sulfo-NHS-LC-LC-Biotin (#21338, Thermo Fisher Scientific) following the manufacturer's instructions, and removal of excessive biotin was performed with Zeba Spin Desalting Columns (7 kDa cut-off, # PI-89883, Thermo Fisher Scientific). Biotinylated Caspr2 protein was coupled with fluorescent neutravidin-labeled beads (ADCD: #F8775; ADCP: #F8776, Thermo Fisher Scientific) at a ratio of 10 μg protein per 10 μL of beads.

Antibody-dependent complement deposition (ADCD)

ADCD was performed following previously established protocol.[48] In brief, patients' sera were heat-inactivated for 30 min at 56°C, diluted 1:20 in 0.1% BSA and then incubated with the coupled antigen beads at 37°C for 2 h. After incubation, unbound antibodies were removed by centrifugation. Guinea pig complement (#CL4051, Cedarlane) was added and incubated at 37°C for 15 min. Next, C3 deposition on the beads was detected using 1:100 diluted FITC conjugated anti-guinea pig C3 polyclonal antibody (#0855385, MP Biomedical) and relative C3 deposition was analyzed by flow cytometry using CytoFLEX (Beckman Coulter). Complement deposition scores were calculated by multiplying the %C3$^+$ beads by the C3$^+$ median fluorescence intensity (MedFI) and dividing by 10^4. A

threshold was set at two times the Standard Error of the Mean (SEM) over the mean of healthy donors (HD) complement deposition scores, and values under this threshold were considered as background and excluded.

Antibody-dependent cellular phagocytosis (ADCP)

ADCP was performed as previously described.[49] In summary, patients' sera were diluted 1:500 and then incubated with the antigen-coupled beads for 2 h at 37°C. After incubation, unbound antibodies were removed by centrifugation and THP-1 monocytes ($2x10^4$ THP-1 cell/well) were added. Following a 4-h incubation period at 37°C, relative phagocytosis was assessed using flow cytometry with CytoFLEX (Beckman Coulter). Phagocytic scores were calculated as the product of the %bead$^+$ THP-1 cells and the median fluorescence intensity (MedFI) of bead$^+$ THP-1 cells, divided by 10^6. A threshold was set at two times the Standard Error of the Mean (SEM) over the mean of healthy donors phagocytic scores, and values under this threshold were considered as background and excluded.

Antibody-dependent NK cell activation (ADNKA)

ADNKA was performed as previously described.[34] ELISA plates were initially coated with 4 μg/mL rhCaspr2 and then blocked with 5% PBS-BSA. Patient's sera, diluted in 1:60, were added to the plates and incubated for 2 h at 37°C. NK cells were isolated from buffy coats of two healthy individuals using the NK isolation Kit (#130–092657, Miltenyi). These cells were cultured in RPMI media supplemented with 1 ng/mL IL-15 at 37°C overnight. Subsequently, NK cells were added to ELISA plates and incubated for 5 h at 37°C with the immunocomplexes, as well as with mouse anti-CD107a (#555802, BD Biosciences), GolgiStop (#554724, BD Biosciences) and brefeldin A (#420601, Biolegend). After incubation, NK cells were surface stained with mouse anti-CD16 (#557758, BD Biosciences), anti-CD56 (#557747, BD Biosciences) and anti-CD3 (#557943, BD Biosciences) antibodies. Cells were fixed and permeabilized using Fix/Perm kit (#00-5523-00, Thermo Fisher Scientific), and subsequently intracellularly stained with mouse anti-MIP-1β (#550078, BD Biosciences), mouse anti-IFN-γ (#554702, BD Biosciences). The NK cells were identified as CD3$^-$CD16$^+$CD56$^+$ cells, and their activation (MIP-1β$^+$, IFN-γ$^+$, CD107a$^+$) was analyzed through flow cytometry with CytoFLEX (Beckman Coulter). Each serum sample was analyzed in parallel using NK cells from both healthy donors. Values from each donor were averaged, and a threshold was set on 2 times the Standard Error of the Mean (SEM) over the mean of the NK activation by serum from HD. Values falling below this threshold were considered background and excluded from analysis.

Fc receptors (FcR) and complement C1q binding

Binding capacity to Fc receptors and C1q complement-binding capacity were measured using a customized singleplex Luminex assay. Briefly, Caspr2 was coupled to fluorescent carboxyl-modified Luminex microspheres. Antigen-coupled microspheres were incubated with serum (dilution 1:80) overnight at 4°C. Immunocomplexes were then washed. Recombinant human FcαR, FcγR2AR, FcγR2AH, FcγR2B, FcγR3AF, FcγR3AV, FcγR3B, and C1q (Duke Protein Production facility) were biotinylated, conjugated to streptavidin-PE, and incubated with the immunocomplexes for 1 h at room temperature. Binding was detected using a Luminex 200 System (R&D system), and Median Fluorescence Intensity (MFI) was reported. Threshold value was set on 2 times the Standard Error of the Mean (SEM) over the mean of the PBS. Values falling below this threshold were considered background and excluded from analysis.

Glycan analyses

Antibody Fc and Fab glycans were analyzed from IgG purified from patients' sera, as follow: IgG Purification. The IgG was isolated using a protein G monolithic (50 μL) plate (BIA Separations). 25 μL of serum was diluted in a ratio 1:7 with 1 × PBS, pH 7.4 and filtered through a 0.45μm AcroPrep wwPTFE filter plate (Pall Corporation). After filtration, serum samples were applied to the protein G plate and washed with 1 × PBS pH 7.4, to remove unbound proteins. IgGs were eluted with 250 μL of 0.1M formic acid (Honeywell) and neutralized with 1M ammonium bicarbonate (Sigma-Aldrich).

Generation of Fc and F(ab')$_2$ fragments

20 μL of CaptureSelect IgG-Fc (Multispecies) beads (Invitrogen, Waltham, MA, USA) were placed in each well of an Orochem filter plate (10 μm pore size, Orochem Technologies) and washed 3 times with 200 μL PBS pH 7.4 on a vacuum manifold. Then, 69.7 μL IgG eluate from most of the samples was applied on the beads. This volume of eluate was calculated based on the average concentration of IgG of the entire cohort which is needed for 50 μg of IgG. However, the eluates of 4 samples had lower IgG concentrations, so instead of 69.7 μL, a larger volume corresponding to 25 μg IgG was applied on the beads. IgG and beads were incubated for 1 h at room temperature on a plate shaker at medium speed. After removal of the ammonium formate, the beads were washed tree times with PBS pH 7.4 and IgG was cleaved into Fc and Fab fragments by the enzyme IdeS (Promega). To each sample, 35 μL PBS pH 6.6 containing 50 U IdeS was added. IgG digestion was performed for 20 h at 37°C in a humidified environment. Fab fragments were collected in a PCR plate after centrifugation at 50 x g for 2 min. Beads were washed 3 times with 200 μL PBS pH 7.4 and 3 times with 200 μL mqH_2O. The Fc fragments were eluted from the beads using 100 μL formic acid and collected in a PCR plate containing 17 μL ammonium bicarbonate after centrifugation at 50 x g for 2 min. Fc and Fab fragments were then dried by vacuum centrifugation.

CGE-LIF analysis of IgG, Fc and Fab glycans

The dried samples were resuspended in 3 μL of 1.66 × PBS and 4 μL 0.5% SDS (Carl Roth, Karlsruhe) and denatured by incubation at 65°C for 10 min. Afterward, 2 μL of 4% Igepal-CA630 (Sigma-Aldrich) was added to each sample and placed on a plate shaker at

medium speed for 5 min. N-glycans were released by adding 1.2 U of PNGase F (Promega) in 1 μL 5 × PBS to each sample and incubated for 3 h at 37°C. Samples were then dried by vacuum centrifugation for 1 h. Dried samples were labeled with 8-aminopyrene-1,3,6-trisulfonic acid (APTS, Synchem) and cleaned by HILIC-SPE on BioGel P10 (Bio-Rad) as described previously.[50]

3 μL of N-glycan post-clean-up eluate and 7 μL Hi-Di Formamide (Applied Biosystems) were pipetted into a MicroAmp Optical 96-well Reaction Plate (Applied Biosystemsand sealed with 96-well plate septa (Applied Biosystems). The xCGE-LIF measurement was performed in a 3500 Genetic Analyzer (Applied Biosystems), equipped with a 50 cm 8-capillary array filled with POP-7 polymer (Applied Biosystems). All samples were run with an oven temperature of 60°C, running voltage of 15 kV and run time of 1000 s. Fab samples were injected for 20 s, and Fc samples were injected for 6 s. Fsa data files were converted to.txt file format using an in-house-developed script and the Empower software (Waters) was used for the integration of the 30 peaks based on previously published data.[51] The abundance of each peak was expressed as a percentage of total integrated area. The composition of N glycan structures in each electrophoretic peak had been assigned previously.[52]

Serologic biomarker assessment

The levels of CD21, CHI3L1, TREM2, CXCL13, IL-15, IL-6 and NfL (pg/mL) in patients' sera were quantified using commercial ELISA assays by Single Plex Assays on Ella Platform (CHI3L1+TREM2: #SPCKC-PS-005492, CD21: #SPCKC-PS-000370, BLA+I-L15+IL6+NFL: #SPCKC-PS-008574, R&D Systems), in accordance with the manufacturer's instructions.

Determination of Caspr2 antibody isotypes

ELISA plates were initially coated with 4 μg/mL rhCaspr2 and then blocked with a solution containing 3% BSA and 0.05% Tween in PBS. Samples' dilutions at 1:100 were added in washing buffer and incubated overnight. After that, mouse biotin-conjugated detection antibodies, targeting human IgG1 (#555869, BD Bioscience, stock: 0.5 mg/mL) and human IgG4 (#555879, BD Bioscience, stock: 0.5 mg/mL), were added at a concentration of 1 μg/mL. After 1h incubation at RT, streptavidin HRP-Conjugate (#18–152, Millipore, 1 μg/mL) was added and incubated for 1h. Finally, TMB substrate was added, and its reaction was stopped with chloric acid. The results were measured at 450 nm, with a reference measurement at 650 nm.

QUANTIFICATION AND STATISTICAL ANALYSIS

Univariate comparisons of antibody features between different groups were conducted using Mann-Whitney U test on GraphPad Prism 9.0.0. Fisher's exact test was applied to analyze differences in clinical features and mRS proportions between groups. Correlations were calculated with Spearman correlation coefficients; p-values <0.05 after Benjamini-Hochberg correction for multiple comparisons were regarded as statistically significant. For multivariate analyses, R software version 4.1.0 was used. Luminex data was logarithmically transformed (log10) and all the features were z-scored. Missing values were imputed using the R package 'missForest'. A partial least squares discriminant analysis (PLSDA) with Least Absolute Shrinkage Selection Operator (LASSO) was applied to select antibody characteristics that most effectively discriminated between the selected groups. The model performance was assessed in a 5-fold cross-validation framework, and the average cross-validation accuracy was reported for 100 repetitions of cross-validation. The model was validated using permutation tests. Control models with ''permuted labels'' were generated, for which the model was trained and applied to data with shuffled group labels in the same cross-validation framework. This procedure was done for 100 permutations for each of 10 cross-validation replicates. The p-values were obtained from the tail probability of the generated null distribution. Receiver operating characteristic (ROC) curves and area under the ROC curve [AUC] were calculated using R to establish sensitivity and specificity of LASSO-selected features in distinguishing LE from non-LE and mild versus severe disease.